Title
Testing microbial models with data from a 14C glucose tracer experiment

Authors
Hagerty, Shannon B
Allison, Steven D
Schimel, Joshua P

Publication Date
2022-09-01

DOI
10.1016/j.soilbio.2022.108781

Peer reviewed

Testing microbial models with data from a ^{14}C glucose tracer experiment

Shannon B. Hagerty, Steven D. Allison, Joshua P. Schimel

Abstract

Most of the carbon (C) that enters the soil is broken down by the microbial community and either respired or stored in soil depending on the microbial allocation strategy. Changes in how the microbial community uses C can significantly affect soil C pool sizes, so new models have begun to explicitly represent microbial allocation. Most models use a parameter called carbon use efficiency (CUE) to represent microbial allocation, which partitions consumed C between respiration and growth. Here we compare a "Typical Microbial Model" with this representation of microbial allocation to two other models. One is the "Microbial Allocation Model" that represents CUE as an emergent property of the microbial community, explicitly modeling multiple processes involved in CUE. The second is the "Two-Pool Biomass Model" that similarly accounts for CUE as an emergent property but also represents the biomass using two C pools with different turnover times. We assessed the models' relative ability to track a ^{14}C-glucose tracer over three weeks through the extractable C pool, the microbial biomass, and respiration. We also used the ^{14}C data to test how estimates of microbial CUE change during the incubation. Our results suggest that CUE estimates in soil are highly sensitive to incubation timing and are at no point stable. Isotopic data can best parameterize models when a time course of measurements is used. Our model comparison showed that the Two-Pool Biomass Model best fit our data. Using the Two-Pool Biomass model to

represent microbial allocation is more biologically realistic and better matches the dynamics observed in our microbial C partitioning data. Biogeochemical models at larger scales may need to consider a dynamic allocation scheme to represent CUE and other microbial parameters rather than assuming they are static values.

Introduction

The future size of the global soil C pool will depend on how microbes such as bacteria and fungi respond to changing environmental conditions (Allison et al., 2010; Wieder et al., 2013; Melillo et al., 2017; Domeignoz-Horta et al., 2020). Microbial communities process most of the C that enters the soil (Cebrian and Lartigue, 2004) and those microbes can alter the fate of that C—whether it is immediately respired or stored —based on their allocation patterns (Six et al., 2006; Sainte-Marie et al., 2021). Microbes have multiple allocation pathways for C: using it for energy, producing enzymes that can accelerate decomposition, building new biomass, or producing exudates that may adhere to soil particles and be stored long-term (Hobbie and Hobbie, 2013; Kallenbach et al., 2016; Liang et al., 2017). Microbial allocation—how C is partitioned across these different pathways—strongly affects the total C balance of the soil (Wieder et al., 2013; Averill, 2014).

Carbon allocation is fundamental to soil organic matter models. Classical models such as CENTURY and ROTH-C assume a defined portion of C moves between soil C-pools and generates respiration (Parton et al., 1987; Jenkinson, 1990). Newly developed models represent microbial partitioning explicitly to better account for microbial

allocation effects on soil C stocks (Schimel and Weintraub, 2003; Allison et al., 2010; Sulman et al., 2014; Wieder et al., 2014; Abramoff et al., 2018). In these models, the microbial biomass or extracellular enzyme pool sizes drive the decomposition rate (Wieder et al., 2015; Wang et al., 2017). Models represent decomposition more realistically this way while also reproducing the global distribution of soil C better than traditional models (Wieder et al., 2013). However, predictions from microbial models depend on how microbial C allocation is represented (Li et al., 2014; Wieder et al., 2017).

Microbial models cannot represent every possible allocation decision; rather, these models aim to include the minimum complexity necessary to predict the bulk effects of microbial processes on soil C storage (Abramoff et al., 2017). Most microbial models aggregate a suite of microbial processes into one parameter that specifies overall carbon use efficiency (CUE), which is the proportion of C uptake used to build new biomass (Bailey et al., 2018; Geyer et al., 2016). CUE is an emergent property that encompasses the respiration necessary to carry out an array of processes: substrate uptake, cell function, enzyme production, cellular maintenance, and exudation (Manzoni et al., 2012; Sinsabaugh et al., 2013; 2016). However in most models, CUE functions more like an assimilation efficiency that simply partitions substrate uptake between biomass and respiration (Ballantyne and Billings, 2018).

The common simplification of microbial allocation into a single CUE term, which only reflects the efficiency of substrate assimilation, causes problems for model predictions and integration with data. Models that use a single CUE parameter have trouble predicting soil C changes when microbial C allocation strategies change in a way unrelated to assimilation efficiency (Hagerty et al., 2018). Additionally, models' CUE

parameters do not aggregate microbial processes in the same way as empirical estimates of CUE. The most common method of estimating CUE involves adding an isotopic C tracer to soil and measuring its partitioning into C pools over some period of time. Previous studies have found that CUE estimates decline over time scales of days or weeks (Ladd et al., 1992; Sugai and Schimel, 1993). This sensitivity is typically attributed to turnover of microbial biomass via predation and regrowth; the effect is assumed to be minimal if CUE is estimated over a short duration (Six et al., 2006). However, we have shown through simulation that estimates of CUE can be sensitive to timing because of cellular processes operating on short time scales (Hagerty et al., 2018). This time-dependence of CUE is inconsistent with using a constant model parameter.

To integrate microbial physiology and ecology with soil organic matter dynamics, models should more effectively capture the dynamics of microbial C allocation processes. We explore two possible approaches. First, models could add additional fluxes of C from the biomass to represent exudation, biomass-specific respiration, and respiration from enzyme production, as in Hagerty et al. (2018). These additional fluxes could provide the model complexity necessary to replicate microbial C partitioning data. A second option would be to represent microbial biomass with two pools; the first representing metabolic constituents that turn over in hours, and the second representing structural C that takes days, weeks, or even longer, to turn over (Glanville et al., 2016). C can be partitioned from either of these biomass pools to other soil C pools.

Several studies have already used such a structure to model C movement through the microbial biomass (Nguyen and Guckert, 2001; Farrar et al., 2012; Glanville et al., 2016). These studies find good agreement with empirical data if microbial C allocation

processes happen in at least two distinct phases. During the first phase, microbes rapidly take up the substrate, assimilating or respiring it. In a second phase, respiration rates decline and the label concentration in the biomass declines more slowly. However, these studies did not compared their two-pool biomass models with other microbial allocation models that might provide even better matches to empirical data.

In this study, we used an isotopic tracer experiment to explore how well different models and parameterizations capture soil C-flow into and through the microbial biomass. First, we aimed to assess microbial C allocation of ^{14}C-glucose added to the soil by tracking the isotope's movement through the extractable C, CO_2, and microbial biomass C (MBC) pools over three weeks. We expected that microbial C allocation would occur in at least two different phases, a fast initial phase followed by a slower secondary phase. We further hypothesized that CUE estimated from the isotopic data would decline over time. Finally, we compared the three microbial models' ability to reproduce the observed patterns in microbial C allocation. We expected that the models representing microbial C allocation with greater process resolution would perform best at capturing the flow C into microbial biomass. In contrast, the *Typical Microbial Model* (TMM), which represents microbial allocation with just a single assimilation efficiency parameter, would have difficulty fitting the ^{14}C data.

Methods

Soil collection and incubation

We collected soil (0-10cm) from the Santa Clara River Valley in California in May 2016. This soil was a Metz loamy sand, classified as a Sandy, mixed, thermic Typic Xerofluvent. Soil was sieved through 2 mm mesh and stored at 4°C until the incubation began a week later. We added soil (15 g dry weight, 62% WHC) to 36 Ball jars and adjusted soil moisture to 42% of the water holding capacity, then pre-incubated the jars in the dark for 7 days.

^{14}C-CO_2 measurements

After the pre-incubation period, four of the jars were sealed, and each cap was fitted with two valves. We then added 1 ml of ^{14}C universally labeled glucose solution (2.4 nmol C or 0.11 μci ml^{-1}) to the soil. Immediately after the glucose solution was added, an air pump with a CO_2 scrubber was connected to one of the valves on each jar. The second valve was connected to three successive CO_2-trapping test tubes that each held 5 ml of 0.5M NaOH, with the last test tube venting out. Air was circulated through the jar into the NaOH traps for one hour. After the hour, an aliquot of each test tube was taken and mixed with scintillation cocktail, counted for ^{14}C activity (on a Beckman 4500 Liquid scintillation counter), then blank and quench corrected. The total ^{14}C concentration in the three traps was used to calculate the ^{14}C-CO_2 production for the first hour. The same four jars were sampled again to measure additional ^{14}C-CO_2 produced at 3 h, 6 h, 24 h, 3 days, 7 days, 14 days, and 21 days. These measurements were used to calculate cumulative $^{14}CO_2$ produced.

^{14}C soil extracts and biomass measurements

We added 1 ml of the same universally labeled ^{14}C-glucose solution to the remaining 32 jars. At each of the previously given time points after label addition, four jars were destructively sampled for extractable C and chloroform fumigation extractable (CFE) biomass. Briefly, half of the soil in the jar was shaken for 30 min with 30 ml of 0.05 M K_2SO_4 and then filtered. The other half of the soil was incubated in the dark for 24 hours with 1 ml of chloroform, and then the K_2SO_4 extraction procedure was repeated. Aliquots of both extracts were mixed with scintillation cocktail and counted like the ^{14}C-CO_2 samples. The microbial biomass ^{14}C concentration was calculated as the difference between the fumigated and unfumigated samples and corrected with the standard correction factor (K_{ec}=0.45) (Brookes et al., 1985). The extractable ^{14}C was considered equivalent to the unfumigated sample ^{14}C concentration.

CUE calculations

To test the influence of timing on CUE measurements, we bootstrapped the data to generate one thousand combinations of replicates from each of the measured pools at every time point. We used the bootstrapped data to calculate microbial CUE at every time point using the three most used equations:

$$CUE_S = (\Delta S - \Delta CO_2^{\square}) / \Delta S \quad (1)$$

$$CUE_B = \Delta B / (\Delta B + \Delta CO_2) \quad (2)$$

$$CUE_C = \Delta B / \Delta S \quad (3)$$

where S, CO_2, and B represent the change in ^{14}C concentration from the initial conditions in the extractable C, CO_2, and microbial biomass pools, respectively. These three equations have each been used in the literature to calculate CUE (Frey et al., 2001), where CUE_S is substrate-based, CUE_B is biomass-based, and CUE_C is concentration based. Most recent studies use CUE_B to estimate CUE (Frey et al., 2013; Kallenbach et al., 2015; Riggs and Hobbie, 2016; Soares and Rousk, 2019).

Models and data fitting

We compared the fit of three different microbial models to the ^{14}C data: a) the Typical Microbial Model, b) the Microbial Allocation Model, and c) Two-Pool Biomass Model (Fig. 1). For each of these models, the Substrate (S) pool was fit to the K_2SO_4 extractable C data, the Biomass pool (B) was fit to the CFE-corrected biomass data, and the CO_2 pool was fit to the $^{14}CO_2$. The difference between the initial amount of labeled C added and the sum of the average label concentrations in each measured pool at each time point was fit to the model's Unextractable pool (U). Because we are modeling the dynamics of ^{14}C glucose, we only included one C substrate pool in all our models. For all models, we fixed the rate that C was taken up from the Extractable pool into the Biomass at 0.9215 h^{-1}, representing the mean proportion of the label that was removed from the extractable C pool 1 hour after addition of the label. Microbial models typically represent uptake as a function of both the substrate pool and the biomass. We have modeled uptake as a function only of the substrate pool size because we assume for a highly labile substrate at a tracer level (i.e., our glucose addition) uptake is constrained only by the concentration of substrate added. The high rate of uptake in the first hour supports this assumption.

Additionally bulk biomass should not change over the first hour, when nearly all uptake occurs, and is unlikely to change over the three-week incubation period. We fit the data to the three models in MATLAB using the Bring Your Own Model (BYOM) software (www.debtox.info/byom.html) developed by Tjalling Jager. BYOM uses a maximum likelihood approach to model fitting. For each model, we calculated Akaike Information Criteria (AIC), a model selection criterion, defined as

$$AIC = 2 * NLL + 2 * k$$

Where *NLL* is the negative log likelihood optimized in the model fitting and *k* is the number of parameters in the model. AIC penalizes models for complexity (Bolker, 2008). To optimize AIC for each model, we removed parameters that did not improve fit. To do this we first fit the model with its full structure (Figure 1), then removed any model fluxes that had rates below 0.001 h^{-1} and refit the modified model (Table 1). If removing the flux minimized AIC because log likelihood was unchanged, but the parameter penalty was reduced, then that flux was left out of the final analysis.

Typical Microbial Model (TMM)

Microbial-explicit models vary widely in how they represent microbial dynamics. We used the basic microbial model structure example from Wieder et al. (2015) as a guide to build our model (Figure 1a). Most importantly, this model represents CUE as an assimilation efficiency parameter that partitions C consumed by microbes between respiration and biomass. The microbial biomass increases as microbes consume the added glucose (S) and convert it into biomass depending on assimilation efficiency. The biomass pool decreases with cell turnover and when C is released to the unextractable

soil C pool (U) or is recycled back to the extractable C pool (S). The differential equation for the biomass pool is therefore:

$$\frac{dB}{dt} = (r_{S,B} * S * ae) - (B * r_{B,U}) \quad (4)$$

where $r_{S,B}$ is the uptake rate (h^{-1}) of the label, ae is assimilation efficiency, and $r_{B,U}$ is the rate of exudation and/or microbial death (h^{-1}). For all parameters representing rate constants, we use the parameter *r* with a subscript indicating the pool C is moving from and the pool it moves into (e.g., parameter $r_{S,B}$ indicates the proportion of C h^{-1} moving from the substrate pool (S) to the biomass pool (B)). Consumed C that is not converted into biomass is respired and the differential equation for the CO_2 pool is:

$$\frac{dC\,O_2}{dt} = ¿ \quad (5)$$

The substrate pool decreases with uptake and increases with recycling from the unextractable pool (U). The differential equation is:

$$\frac{dS}{dt} = -(r_{S,B} * S) + (U * r_{U,S}) \quad (6)$$

Microbial products move to the unextractable pool, and this pool decreases when C is lost at a constant rate ($r_{U,S}$; h^{-1}) and recycled back into the substrate pool. The differential equation for this unextractable pool is therefore:

$$\frac{dU}{dt} = B * r_{B,U} - U * r_{U,S} \quad (7)$$

Microbial Allocation Model (MAM)

We fit the data to a modified version of the microbial-explicit model from Hagerty et al. (2018). In this version, CUE is an emergent property—the model explicitly represents several C-allocation processes, and the overall CUE represents the integrated effect of all these processes. Microbes take up C and then split it three ways between the biomass based on assimilation efficiency (*ae*), the unextractable pool determined by the parameter *es,* and the remaining C that is respired. We also explicitly represent microbial maintenance respiration which occurs as a proportion of the biomass ($r_{B,CO2}$; h^{-1}). The differential equation for CO_2 is then:

$$\frac{dC\,O_2}{dt} = ¿ \quad (8)$$

This modification affects the differential equation for the biomass:

$$\frac{dB}{dt} = (r_{S,B} * S * ae) - (B * r_{B,U}) - (B * r_{B,CO2}) \quad (9)$$

and the equation for the unextractable pool is now:

$$\frac{dU}{dt} = (r_{S,B} * S * es) - (U * r_{U,S}) + (B * r_{B,U}) \quad (10)$$

The differential equation for the substrate pool is the same as in the typical microbial-explicit model (eqn. 6).

Two-Pool Biomass Model (TPBM)

We also used a model that represents the biomass in two pools, a metabolic biomass C pool (MB) and a structural biomass C pool (SB). This two-pool structure allows the different components of the biomass to turn over at different rates. This model formulation is like the microbial allocation model: CUE becomes an emergent property, rather than being a pre-assigned value. The biomass takes up C and assimilates it into the MB pool. From the MB pool, C can be respired at a rate $r_{MB,CO2}$, lost from the cell with exudation at a rate $r_{MB,U}$, or converted into structural biomass at a rate $r_{MB,SB}$. The differential equation for the MB pool is then:

$$\frac{dMB}{dt} = (r_{S,MB} * S) - (MB * r_{MB,SB}) - (MB * r_{MB,CO2}) - (MB * r_{MB,U}) \quad (10)$$

C is converted from MB to SB, increasing the SB pool. The SB pool decreases when C is respired through maintenance respiration ($r_{SB,CO2}$). The differential equation for SB is then:

$$\frac{dSB}{dt} = (MB * r_{MB,SB}) - (SB * r_{SB,CO2}) - (SB * r_{SB,U}) \quad (11)$$

263 We fit the total microbial biomass (B) to the CFE biomass data. The total microbial
264 biomass pool is equivalent to the sum of the SB and MB pools. The sum increases with
265 uptake and decreases as C is respired from the structural or metabolic pools or as
266 exudation occurs. The differential equation for the biomass pool is then:
267
268 $$\frac{dB}{dt}=(r_{S,MB}*S)-(MB*r_{MB,CO2})-(MB*r_{MB,U})-(SB*r_{SB,U})-(SB*r_{SB,CO2})$$
269 (12)
270 and the differential equation for CO_2 is:
271
272 $$\frac{dCO2}{dt}=(MB*r_{MB,CO2})+(SB*r_{SB,CO2})$$ (13)
273
274 Exudation from the MB pool and death from the SB pool increase the unextractable C
275 pool (U), while recycling of C back to the substrate pool decreases U.
276
277 $$\frac{dU}{dt}=(MB*r_{MB,U})+(SB*r_{SB,U})-(U*r_{U,S})$$ (14)
278
279 The differential equation for the substrate pool is similar to the other two models, but
280 the rate constant parameter notation for uptake is $r_{S,MB}$. The C leaving the substrate pool
281 goes to the MB pool.
282
283 $$\frac{dS}{dt}=-(r_{S,MB}*S)+(U*r_{U,S})$$

Results

Microbial ^{14}C glucose allocation patterns

The ^{14}C was rapidly assimilated into the microbial biomass; within the first hour after addition, microbes had taken up 91% of the added label. At that time, 78% was in the microbial biomass, 7% had been respired, and the remaining 7% was unrecoverable in the unextractable pool (Figure 2). From hour 1 to hour 72, the concentration of the label in the biomass declined while the amounts respired and in the unextractable pool increased. After 72 hours, until the end of the incubation, the proportion of the label in the biomass continued to decrease while the proportion in CO_2 increased, but at much lower rates. The amount of label in the unextractable pool remained stable during this period. By the end of the incubation at 21 days, 31.6% of the label added was in the unextractable pool, 38.5% was in the biomass, 29.6% had been respired, and <1% was in the extractable C pool.

CUE estimates and model parameters

Calculated values of CUE responded non-linearly to incubation time (Figure 3). At 1 hour, mean CUE_S, $CUE_{B,}$ and CUE_C were 0.93, 0.92, and 0.85 respectively. These estimates rapidly declined over the first 72 hours to 0.74, 0.59, and 0.34, with rates of decline slowing with time. After 72 hours the CUE estimates were relatively stable and at the end of the incubation CUE_S was as 0.70, CUE_B was 0.56, and CUE_C was 0.39.

Model parameter estimates for the Typical Microbial Model, Microbial Allocation Model, and the Two-Pool Biomass Model are in Tables 2, 3, and 4 respectively. In the Typical Microbial Model, assimilation efficiency was 0.84 mg C mg^{-1} C. This value was higher than the assimilation efficiency value of 0.59 mg C mg^{-1} C in the Microbial Allocation Model. The Microbial Allocation Model parameter $r_{B,CO2}$ value was close to the Two-Pool Biomass Model parameter $r_{SB,CO2}$. For these two parameters, the confidence intervals overlapped. In the Two-Pool Biomass Model, the parameter values indicated that the largest flux of C leaving the MB pool is directed toward the SB pool and the smallest converts MB to CO_2. After C enters the SB pool it moves to CO_2 or U at similar rates, although there was higher uncertainty around the estimate for $r_{SB,U}$.

Comparison of model fits to ^{14}C data

When we fit the different microbial models to the ^{14}C data (Figure 2), we found that removing the flux of C from the unextractable pool to the substrate pool minimized AIC (Table 1) for the Microbial Allocation Model and the Two-Pool Biomass Model. Consequently, we did not estimate a parameter value for $r_{U,S}$ for either of these models. Additionally for the Microbial Allocation Model, AIC was further minimized by removing the flux of C that directed a proportion of the biomass to the unextractable pool at each time step, so we did not fit parameter $r_{B,U}$ for this model. The model equations can be updated to account for these changes by using 0 as the parameter value for the unfit parameters. Figure 1 shows the final model structures.

The Two-Pool Biomass model had the lowest AIC value, indicating this model fit the data best, followed by the Microbial Allocation Model; while the Typical Microbial

Model did the worst (Table 1). The most notable difference in model performance was in the fit to the ^{14}C biomass dynamics. The Two-Pool Biomass Model reproduced the ^{14}C dynamics as it moved through the biomass with the lowest model error at every time point (Figure 4). All the models underestimated the initial amount of ^{14}C in the biomass at the first hour by 32, 37, and 55% for the Two-Pool Biomass Model, Microbial Allocation Model, and Typical Microbial Model respectively. The models had the greatest divergence in their ability to replicate the decrease of ^{14}C-MBC from 1 to 24h. The Two-Pool Biomass Model best matched this pattern. The Typical Microbial Model underestimated the rate of decline while the Microbial Allocation Model underestimated the initial biomass so that it missed that this phase entirely. The models varied in their abilities to reproduce ^{14}C patterns in the unextractable pool. The Typical Microbial Model underestimated ^{14}C in the unextractable pool from 1 to 72 hours and then overestimated from hour 72 until the end of the incubation. The Microbial Allocation Model overestimated the ^{14}C in the unextractable pool from 1 to 24h, and then underestimated the concentration from 72 h on. The Two-Pool Biomass model matched the pattern of the unextractable pool better with the lowest error at every time point except for hour 6.

All three models' estimates of CO_2 production had the largest error early in the incubation. The Typical Microbial Model and Microbial Allocation Model overestimated respiration during this time while the Two-Pool Biomass model underestimated it. However, after 6 hours, all three models estimated values within 20% of the measured value throughout the incubation. The models fit the data similarly for the extractable C pool; all three models predicted less than 1% of the label remained in the extractable pool by 24h consequently absolute differences between model predictions were negligible.

Discussion

Microbial allocation of ^{14}C-glucose

We hypothesized that allocation of the ^{14}C-glucose tracer would occur in at least two phases. Our ^{14}C allocation data supported this hypothesis, showing that microbial C partitioning is highly dynamic over time. Specifically, we observed three phases of microbial C allocation during the three-week incubation. The initial phase was characterized by microbial assimilation. During the first hour following the label addition, ^{14}C was rapidly taken up into the microbial biomass, while being depleted from the extractable pool. During this phase, there was rapid respiration of $^{14}CO_2$ but the total amount of ^{14}C respired was still limited (<20%); most of the label was in the biomass. This pattern reflects the high efficiency of microbial assimilation of labile substrates such as glucose (Ladd et al., 1992; Sugai and Schimel, 1993).

The second phase began after the first hour and continued until 24 h. During this time, there was a rapid decline of the ^{14}C label in biomass, high ^{14}C-CO_2 production, and ^{14}C movement into the unextractable pool. Other studies have observed a similar proportion of ^{14}C in the unextractable pool (Witter and Dahlin, 1995; Nguyen and Guckert, 2001). The synchronized decline in the label in the biomass and increase of label in the unextractable C pools indicates products released from microbial cells were entering the soil matrix. Microbial exudation occurs as microbes create and release extracellular products including enzymes, antibiotics, or polysaccharides (Sinsabaugh and Shah, 2012; Basler et al., 2015; Tyc et al., 2016). Microbes release metabolic by-products

373 when metabolites are in excess or when metabolic pathways shift rendering the
374 metabolite unnecessary (Varma and Palsson, 1994). By-products can be released at a per-
375 mole rate that is up to 40% the rate of glucose uptake in culture where glucose is the sole
376 C source (Fuhrer et al., 2005), meaning that exudation could be a significant flux of C
377 from the biomass. Yet with the exception of extracellular enzyme production, microbial
378 exudation is typically ignored in microbial models. Microbial exudates can affect model
379 projections for soil C stock size (Hagerty et al., 2018) and could be an important
380 mechanism directing C to long-term storage in soil (Liang et al., 2017).
381 The third phase of microbial allocation began 24 h into the incubation and
382 continued until the end of the experiment. During this phase, microbes lost ^{14}C from the
383 biomass and respired ^{14}C slowly. During this period, the dominant C-flux is microbial
384 biomass to CO_2, likely because of cellular maintenance processes and community
385 dynamics such as grazing and microbial death.
386
387 *CUE estimates and model parameter values*
388 A key focus of this research was to evaluate three different microbial models and
389 to compare their skill in replicating C allocation patterns. Empirical CUE estimates were
390 sensitive to the duration of the experiment and were not stable at any point (Figure 3).
391 These results contrast with the assumption that community turnover causes estimated
392 CUE to decline linearly and slowly (Hagerty et al., 2014). Rather, our CUE estimates
393 declined nonlinearly, and declined most rapidly from 1 h to 24 h after addition of the
394 label. CUE metrics based on the ^{14}C concentration in the microbial biomass (i.e., CUE_B
395 and CUE_C) followed a pattern over time complementary to the biomass pattern. We also

observed this pattern with CUE_S, although the rate of change was slower (Figure 3). The measured decline in CUE reflects the ongoing loss of ^{14}C to $^{14}CO_2$ and was observed regardless of the CUE metric.

Because CUE estimates varied with time, a single value cannot be used to parameterize models. While the Typical Microbial Model assimilation efficiency was comparable to the 1h CUE estimate, for the Microbial Allocation Model, the assimilation efficiency was lower and more closely related to the CUE estimates after 24h. CUE estimates declined as more cellular processes were incorporated into the measurement, reducing the label concentration in the biomass. The Microbial Allocation Model had a lower assimilation efficiency because it includes exudation, unlike the Typical Microbial Model. The Two-Pool Biomass Model does not instantaneously partition C; instead C enters the metabolic biomass pool and is then directed to another pool as a function of the metabolic biomass pool size. The ratio of the three rate constants that direct C out of this pool was similar to the partitioning of C with uptake in the Microbial Allocation Model. The structural biomass pool in the Two-Pool Biomass Model and the biomass pool in the Microbial Allocation Model had similar rates for CO_2 production. These parameter comparisons suggest that the structural biomass pool is approximating the behavior of a single microbial biomass pool in the Microbial Allocation Model.

Microbial C allocation model selection

By comparing models, we aimed to determine the most effective approach for representing microbial C partitioning. Existing models generally aggregate all microbial allocation into one CUE parameter that instantaneously partitions consumed C. We

419 expected that the model with this structure (i.e., the Typical Microbial Model) would
420 have difficulty matching our empirical data. AIC values supported this prediction and
421 indicated that the Two-Pool Biomass Model best fit our data, though the improvement
422 was modest. However, the advantage of the Two-Pool Biomass Model grows when we
423 also consider biological interpretability. Biological interpretability ensures that models
424 relate meaningfully to both theory *and* measurements. A tight connection between
425 mathematical models, theory, and measurements has been a factor in the widespread
426 adoption and longevity of existing soil C models (e.g. Century and ROTH-C), and will
427 likely be critical for the success of new microbial models (Blankinship et al., 2018).
428 As opposed to the typical single-parameter representation of microbial allocation
429 in most models, the Two-Pool Biomass Model represents CUE as an emergent property
430 that is a function of microbial allocation processes. Such a representation of microbial
431 allocation may ultimately lead to better soil C model predictions because models can
432 account for a wider range of effects on C cycling with shifts in microbial allocation
433 (Hagerty et al., 2018). For example, with substrates that get sorbed or react abiotically,
434 the two pool model might better capture competition between uptake and sorption or
435 reaction. That model might also facilitate incorporating stoichiometric influences on CUE
436 (Sinsabaugh et al., 2016). Like our glucose substrate, C-rich compounds might be taken
437 up rapidly and then be respired via overflow metabolism (Schimel and Weintraub, 2003)
438 to maintain the C:nutrient ratio of biomass.
439 Representing biomass with two pools also addresses two additional issues with
440 existing microbial models. First, in most microbial models, C is respired without ever
441 entering the biomass (Ballantyne, 2018). In the Two-Pool Biomass Model, C must enter

442 the metabolic pool before it can be respired. The second issue relates to how the size of
443 the biomass pool controls the decomposition rate. In typical microbial models, changes in
444 the microbial biomass pool size affect substrate uptake rate (Allison et al., 2010; Wang et
445 al., 2013; Wieder et al., 2015). However, in our analysis, the Typical Microbial Model
446 does not account for all microbial C losses, resulting in an overestimated biomass pool
447 size from 3 to 72 h. During the same time, the model underestimated the amount of
448 biomass C being directed to the unextractable pool. If this model were to be used at larger
449 scales of space and time, these incorrect biomass dynamics might result in overestimated
450 decomposition rates and underestimated soil C stocks. Although we did not consider this
451 effect in our short-term simulations, the Two-Pool Biomass Model could easily represent
452 such feedbacks in longer simulations.

453 The two-pool representation of microbial biomass is also an improvement
454 because it can distinguish between C that has just been assimilated from C that represents
455 new growth. The two biomass pools can be interpreted as representing the labile or
456 metabolic biomass in the first microbial pool and the structural microbial C in the second
457 pool. The structural pool will likely be indicative of changes in microbial cells,
458 correlating with changes in the abundance of decomposers. It may be more appropriate to
459 use structural biomass than the total biomass pool size when scaling cellular uptake rates.
460 With the two-pool biomass structure, the model can account for the fact that recently
461 assimilated C is within the biomass pool but has not yet been incorporated into cell
462 physiological machinery and should not be part of the pool controlling decomposition
463 rates. This distinction may be particularly important in models where the size of the
464 enzyme pool controls decomposition rates. In these models, enzymes are usually

produced as a function of the biomass pool size (Allison et al., 2010; Wang et al., 2013). Overestimating biomass would therefore also overestimate enzyme production and decomposition.

Conclusions

Our results highlight a disconnect between reality and model representations of how microbes allocate C among different fates. Models representing CUE as an emergent property of multiple microbial processes, as opposed to a single parameter, best match our C partitioning data and theoretical understanding of microbial C use. Our study also demonstrates how isotopic partitioning data collected over time can be used to parameterize microbial models. This approach will more accurately constrain microbial allocation parameters compared to a single time point. The Two-Pool Biomass Model fit our data better than either the Typical Microbial Model or the Microbial Allocation Model. We propose that considering microbial allocation within the framework of the Two-Pool Biomass Model could allow for better integration of empirical data into soil C models and greater confidence that microbial allocation effects on soil C stock size are appropriately constrained.

References

Abramoff, R., Z., A. Davidson Eric, and C. Finzi Adrien. 2017. A parsimonious modular approach to building a mechanistic belowground carbon and nitrogen model. Journal of Geophysical Research: Biogeosciences 122, 2418-2434.

Abramoff R., Xu X., Hartman M., O'Brien S., Feng W., Davidson, E., Finzi, A., Moorhead, D., Schimel, J., Torn, M., Mayes, M.A. 2017. The Millennial model: in search of measurable pools and transformations for modeling soil carbon in the new century. Biogeochemistry 137, 51-71.

Allison, S. D., Wallenstein, M. D., Bradford, M. A. 2010. Soil-carbon response to warming dependent on microbial physiology. Nature Geoscience 3, 336-340.

Averill, C. 2014. Divergence in plant and microbial allocation strategies explains continental patterns in microbial allocation and biogeochemical fluxes. Ecology Letters 17, 1202-1210.

Bailey, V. L., Bond-Lamberty, B., DeAngelis, K., Grandy, A. S., Hawkes, C. V., Heckman, K., Lajtha, K., Phillips, R. P., Sulman, B. N., Todd-Brown, K. E. O., Wallenstein, M. D. 2018. Soil carbon cycling proxies: Understanding their critical role in predicting climate change feedbacks. Global Change Biology 24, 895-905.

Ballantyne, F., Billings, S. A. 2018. Model formulation of microbial CO2 production and efficiency can significantly influence short and long term soil C projections. The ISME journal.

Basler, A., Dippold, M., Helfrich, M., Dyckmans, J. 2015. Microbial carbon recycling, an underestimated process controlling soil carbon dynamics. Biogeosciences Discussions 12.

Blankinship, J. C., Berhe, A. A., Crow, S. E., Druhan, J. L., Heckman, K. A., Keiluweit, M., Lawrence, C. R., Marín-Spiotta, E., Plante, A. F., Rasmussen, C., Schädel, C., Schimel, J. P., Sierra, C. A., Thompson, A., Wagai, R., Wieder, W. R. 2018.

509 Improving understanding of soil organic matter dynamics by triangulating
510 theories, measurements, and models. Biogeochemistry 140, 1-13.
511 Bolker, B. M. 2008. Ecological Models and Data in R. Princeton University Press.
512 Brookes, P. C., Landman, A., Pruden, G., Jenkinson, D. S. 1985. Chloroform fumigation
513 and the release of soil-nitrogen - a rapid direct extraction method to measure
514 microbial biomass nitrogen in soil. Soil Biology & Biochemistry 17, 837-842.
515 Domeignoz-Horta, L.A. Pold, G., Liu, X.-J. A., Frey, S.D., Melillo, J.M., DeAngelis,
516 K.M. 2020. Microbial diversity drives carbon use efficiency in a model soil.
517 Nature Communications 11:3684.
518 Cebrian, J., Lartigue, J. 2004. Patterns of herbivory and decomposition in aquatic and
519 terrestrial ecosystems. Ecological Monographs 74, 237-259.
520 Farrar, J., Boddy, E., Hill, P. W., Jones, D. L. 2012. Discrete functional pools of soil
521 organic matter in a UK grassland soil are differentially affected by temperature
522 and priming. Soil Biology and Biochemistry 49, 52-60.
523 Frey, S. D., Gupta, V., Elliott, E. T., Paustian, K. 2001. Protozoan grazing affects
524 estimates of carbon utilization efficiency of the soil microbial community. Soil
525 Biology & Biochemistry 33, 1759-1768.
526 Frey, S. D., Lee, J., Melillo, J. M., Six, J. 2013. The temperature response of soil
527 microbial efficiency and its feedback to climate. Nature Climate Change 3, 395-
528 398.
529 Fuhrer, T., Fischer, E., Sauer, U. 2005. Experimental identification and quantification of
530 glucose metabolism in seven bacterial species. Journal of Bacteriology 187, 1581-
531 1590.
532 Geyer, K. M., Kyker-Snowman, E., Grandy, A. S., Frey, S. D. 2016. Microbial carbon
533 use efficiency: accounting for population, community, and ecosystem-scale
534 controls over the fate of metabolized organic matter. Biogeochemistry 127, 173-
535 188.
536 Glanville, H. C., Hill, P. W., Schnepf, A., Oburger, E., Jones, D. L. 2016. Combined use
537 of empirical data and mathematical modelling to better estimate the microbial

538 turnover of isotopically labelled carbon substrates in soil. Soil Biology and
539 Biochemistry 94, 154-168.
540 Hagerty, S. B., van Groenigen, K. J., Allison, S. D., Hungate, B. A., Schwartz, E., Koch,
541 G. W., Kolka, R. K., Dijkstra, P. 2014. Accelerated microbial turnover but
542 constant growth efficiency with warming in soil. Nature Climate Change 4, 903-
543 906.
544 Hobbie, J. E., Hobbie, E. A. 2013. Microbes in nature are limited by carbon and energy:
545 the starving-survival lifestyle in soil and consequences for estimating microbial
546 rates. Frontiers in Microbiology 4.
547 Jenkinson, D.S. 1990. The turnover of organic carbon and nitrogen in soil. Philosophical
548 Transactions of the Royal Society of London 329, 361-368.
549 Kallenbach, C., Grandy, A., Frey, S., Diefendorf, A. 2015. Microbial physiology and
550 necromass regulate agricultural soil carbon accumulation. Soil Biology and
551 Biochemistry 91, 279-290.
552 Kallenbach, C. M., Frey, S. D., Grandy, A. S. 2016. Direct evidence for microbial-
553 derived soil organic matter formation and its ecophysiological controls. Nature
554 Communications 7, 13630.
555 Ladd, J. N., Jocteur-Monrozier, L., Amato, M. 1992. Carbon turnover and nitrogen
556 transformations in an alfisol and vertisol amended with [U-14C] glucose and
557 [15N] ammonium sulfate. Soil Biology and Biochemistry 24, 359-371.
558 Li, J. W., Wang, G. S., Allison, S. D., Mayes, M. A., Luo, Y. Q. 2014. Soil carbon
559 sensitivity to temperature and carbon use efficiency compared across microbial-
560 ecosystem models of varying complexity. Biogeochemistry 119, 67-84.
561 Liang, C., Schimel, J., Jastrow, J. 2017. The importance of anabolism in microbial
562 control over soil carbon storage. Nature Microbiology 2, 17105.
563 Manzoni, S., Taylor, P., Richter, A., Porporato, A., Agren, G. I. 2012. Environmental and
564 stoichiometric controls on microbial carbon-use efficiency in soils. New
565 Phytologist 196, 79-91.
566 Melillo, J. M., Frey, S. D., DeAngelis, K. M., Werner, W. J., Bernard, M. J., Bowles, F.
567 P., Pold, G., Knorr, M. A., Grandy, A. S. 2017. Long-term pattern and magnitude

568 of soil carbon feedback to the climate system in a warming world. Science 358,
569 101-105.
570 Nguyen, C., Guckert, A. 2001. Short-term utilisation of 14C-[U]glucose by soil
571 microorganisms in relation to carbon availability. Soil Biology and Biochemistry
572 33, 53-60.
573 Parton, W.J. Schimel, D.S., Cole, C.V., Ojima, D.S. 1987. Analysis of factors controlling
574 soil organic matter levels in Great Plains grasslands. Soil Science Society of
575 America Journal 51, 1173-1179.
576 Riggs, C. E., Hobbie, S. E. 2016. Mechanisms driving the soil organic matter
577 decomposition response to nitrogen enrichment in grassland soils. Soil Biology
578 and Biochemistry 99, 54-65.
579 Sainte-Marie J., Barrandon M., Saint-André L., Gelhaye E., Martin F., Derrien D. 2021.
580 C-STABILITY an innovative modeling framework to leverage the continuous
581 representation of organic matter. Nature Communications 12, 1–13.
582 Schimel, J. P., Weintraub, M. N. 2003. The implications of exoenzyme activity on
583 microbial carbon and nitrogen limitation in soil: a theoretical model. Soil Biology
584 and Biochemistry 35, 549-563.
585 Sinsabaugh, R. L., Manzoni, S., Moorhead, D. L., Richter, A. 2013. Carbon use
586 efficiency of microbial communities: stoichiometry, methodology and modelling.
587 Ecology Letters 16, 930-939.
588 Sinsabaugh, R. L., Shah, J. J. F. 2012. Ecoenzymatic Stoichiometry and Ecological
589 Theory. Annual Review of Ecology, Evolution, and Systematics 43, 313-343.
590 Sinsabaugh, R.L., Turner, J.M., Talbot, J., Waring, B.G., Powers, J.S., Kuske, C.R.,
591 Moorhead, D.L., Follstad Shah, J.J., 2016. Stoichiometry of microbial carbin use
592 efficiency in soils. Ecological Monographs 86, 172–189.
593 Six, J. Frey, S. D., Thiet, R. K., Batten, K. M. 2006. Bacterial and fungal contributions to
594 carbon sequestration in agroecosystems. Soil Science Society of America Journal
595 70, 555-569.

596 Sugai, S. F., Schimel, J. P. 1993. Decomposition and biomass incorporation of C-14-
597 labeled glucose and phenolics in taiga forest floor - effect of substrate quality,
598 successional state, and season. Soil Biology & Biochemistry 25, 1379-1389.
599 Sulman, B. N., Phillips, R. P., Oishi, A. C., Shevliakova, E., Pacala, S. W. 2014.
600 Microbe-driven turnover offsets mineral-mediated storage of soil carbon under
601 elevated CO_2. Nature Climate Change 4, 1099.
602 Tyc, O., Song, C., Dickschat, J. S., Vos, M., Garbeva, P. 2016. The Ecological Role of
603 Volatile and Soluble Secondary Metabolites Produced by Soil Bacteria. Trends in
604 Microbiology 25, 280-292.
605 Varma, A., Palsson, B. O. 1994. Stoichiometric flux balance models quantitatively
606 predict growth and metabolic by-product secretion in wild-type escherichia-coli
607 w3110. Applied and environmental microbiology 60, 3724-3731.
608 Wang, G. S., Post, W. M., Mayes, M. A. 2013. Development of microbial-enzyme-
609 mediated decomposition model parameters through steady-state and dynamic
610 analyses. Ecological Applications 23, 255-272.
611 Wang, K., Peng, C., Zhu, Q., Zhou, X., Wang, M., Zhang, K., Wang, G. 2017. Modeling
612 Global Soil Carbon and Soil Microbial Carbon by Integrating Microbial Processes
613 into the Ecosystem Process Model TRIPLEX-GHG. Journal of Advances in
614 Modeling Earth Systems 9, 2368-2384.
615 Wieder, W., Grandy, A., Kallenbach, C., Bonan, G. 2014. Integrating microbial
616 physiology and physio-chemical principles in soils with the MIcrobial-MIneral
617 Carbon Stabilization (MIMICS) model. Biogeosciences 11, 3899-3917.
618 Wieder, W., R., Hartman M. D., Sulman B. N., Wang, Y-. P., Koven C. D., Bonan G. B.
619 2017. Carbon cycle confidence and uncertainty: Exploring variation among soil
620 biogeochemical models. Global Change Biology 24, 1563-1579.
621 Wieder, W. R., Allison, S. D., Davidson, E. A., Georgiou, K., Hararuk, O., He, Y.,
622 Hopkins, F., Luo, Y., Smith, M. J., Sulman, B. 2015. Explicitly representing soil
623 microbial processes in Earth system models. Global Biogeochemical Cycles 29,
624 1782-1800.

625 Wieder, W. R., Bonan, G. B., Allison, S. D. 2013. Global soil carbon projections are
626 improved by modelling microbial processes. Nature Climate Change 3, 909-912.
627 Witter, E., Dahlin, S. 1995. Microbial utilization of [U-14C]-labelled straw and [U-13C]-
628 labelled glucose in soils of contrasting pH and metal status. Soil Biology and
629 Biochemistry 27,1507-1516.
630

631 Table 1. Model AIC values. For each model we estimated parameters using the structure

632 that minimized AIC. The lowest value for each model is in bold.

Model Structure	Typical Microbial Model	Microbial Allocation Model	Two-Pool Biomass Model
Full Structure	**-417.7**	-422.0	-463.8
Without $r_{U,S}$	--	-424.0	**-465.8**
Without $r_{B,U}$	--	-424.0	-462.4
Without $r_{U,S}$ or $r_{B,U}$	--	**-426.0**	-464.4

633

634

635 Table 2. Typical Microbial Model best fit parameter estimates and confidence interval.

Parameter	Value	CI	Units
$r_{B,U}$	6.7 x 10^{-3}	4.9x10^{-3}-9.1 x 10^{-3}	h^{-1}
$r_{U,S}$	6.2 x10^{-3}	4.3x10^{-3}-8.9x10^{-3}	h^{-1}
$r_{S,B}$	0.84	0.82-0.86	mg C mg^{-1} C

636

637

638 Table 3. Microbial Allocation Model best fit parameter estimates and confidence

639 intervals.

Parameter	Value	CI	Units
ae	0.59	0.53-0.64	mg C mg^{-1}
es	0.25	0.20-0.31	mg C mg^{-1}
$r_{B,CO2}$	6.5 x 10^{-4}	$5.3x10^{-4}$-$8.0x10^{-4}$	h^{-1}

640

641

642 Table 4. Two-Pool Biomass Model best fit parameter estimates and confidence intervals.

Parameter	Value	CI	Units
$r_{MB,SB}$	0.27	0.17-0.49	h^{-1}
$r_{MB,CO2}$	0.089	0.063-0.14	h^{-1}
$r_{MB,U}$	0.12	0.078-0.18	h^{-1}
$r_{SB,CO2}$	$5.4x10^{-4}$	$4.1x10^{-4}$-$6.9x10^{-4}$	h^{-1}
$r_{SB,U}$	$5.5x10^{-4}$	0-$1.3x10^{-3}$	h^{-1}

643

644

645

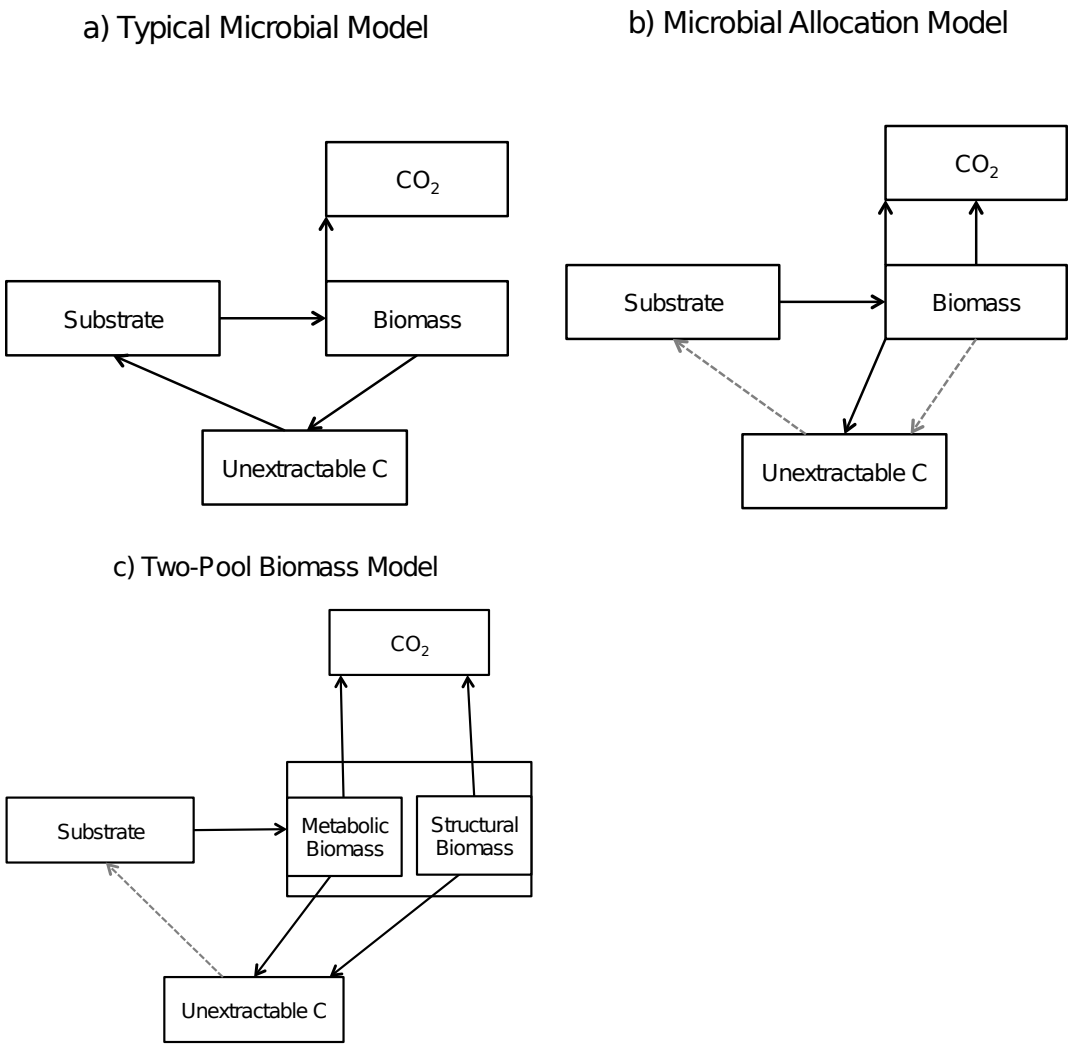

646

647

648

649 Figure 1. Model structures for a) Typical Microbial Model, b) Microbial Allocation
650 Model, c) Two-Pool Biomass Model. For each model the Extractable C, Biomass, and
651 CO_2 pools were fit to experimental data and the unextractable pools were fit to the mean
652 concentration of the label unrecovered, calculated as the difference between the label
653 added and the sum of the averages for each of the three measured pools at each time
654 point. Grey dashed lines represent fluxes that were found to be unnecessary for the model
655 to fit the data. In the Typical Microbial Model and the Microbial Allocation Model fluxes
656 positioned at the boundary of the biomass pool occur as a function of substrate uptake; all
657 other arrows represent fluxes that occur as a proportion of its origin pool.
658

659

660

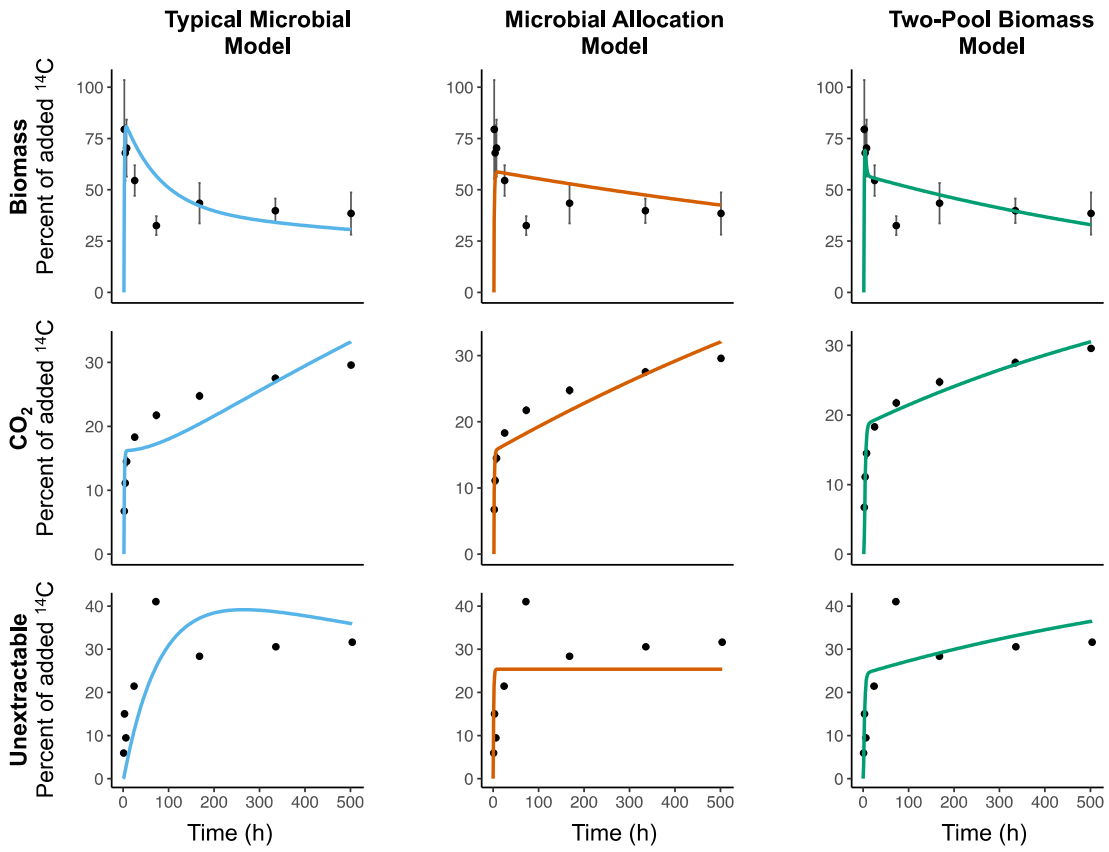

661 Figure 2. Fit of the Typical Microbial Model (blue line), Microbial Allocation Model (red
662 line), and Two Pool biomass Model (green line) to the experimental ^{14}C data for the
663 microbial biomass, CO_2 and unextractable C pools. For the biomass and CO_2 plots, points
664 represent mean and error bars represent standard deviation. The unextractable pool was
665 calculated as the difference between the amount of ^{14}C added and the mean amount
666 recovered in the CO_2, extractable, and biomass pools.
667

668

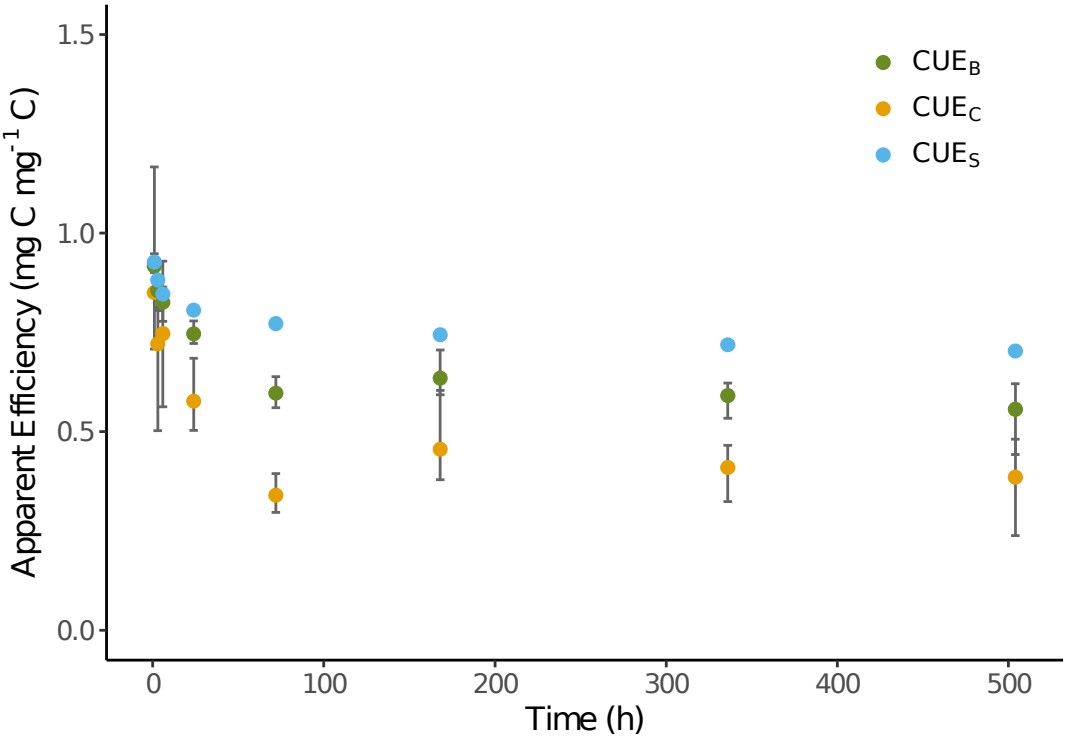

669

670 Figure 3. CUE estimated from isotopic pools over time. Concentrations of ^{14}C in each C
671 pool at each time point were bootstrapped to produce 1000 combinations of the three
672 measured pools at each time point and then used to calculate CUE. Points represent
673 means and error bars represent 95% confidence interval.

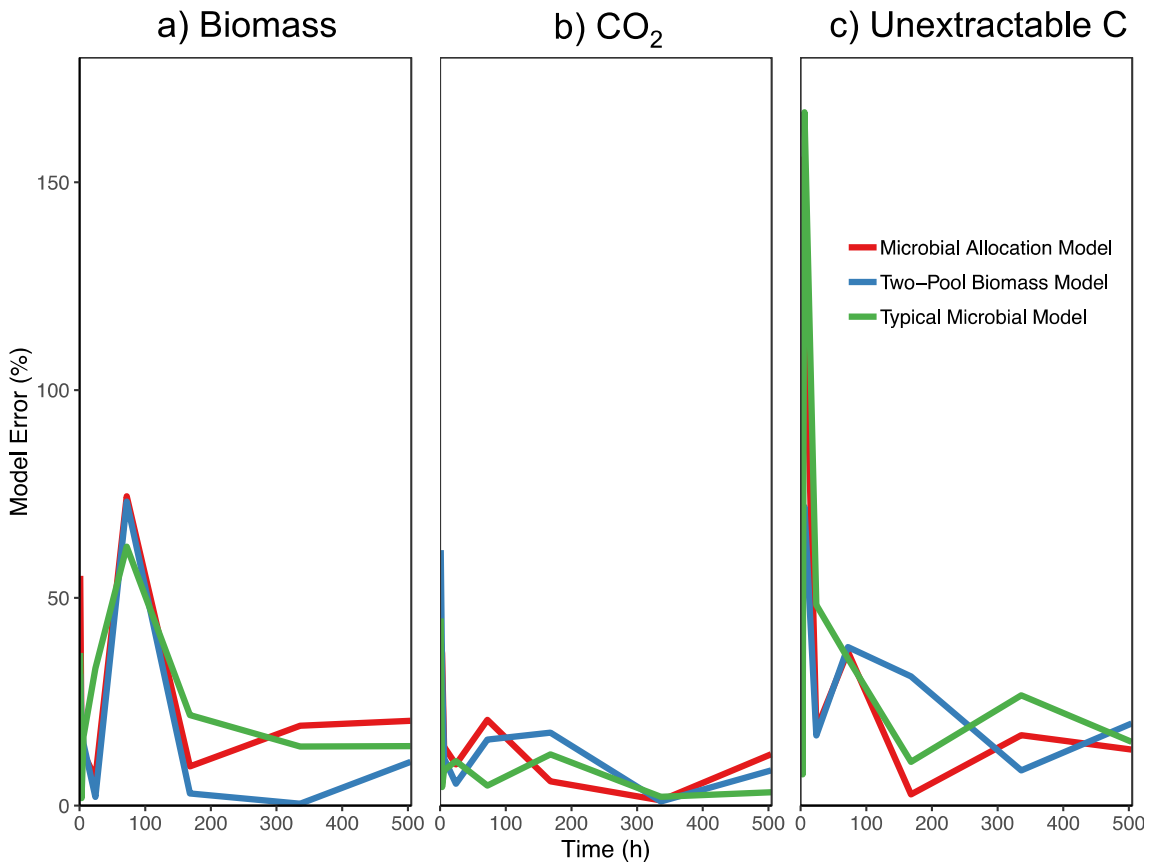

675 Figure 4. Model error over the course of the incubation for the a) Biomass, b) CO_2, and c)
676 Unextractable C pools for the Microbial Allocation Model, Two-Pool Biomass Model,
677 and Typical Microbial Model. Model error is calculated as the absolute value of the
678 difference between the model estimate of ^{14}C in the pool and the measured concentration
679 of the label in the pool, divided by the measured value. After one hour, the amount label
680 in the extractable C pool was less than 8% and declined to less 1% of the total amount
681 added to soil by the end of the incubation. Because the absolute amount of ^{14}C in this
682 pool was so low, model error was high for all models and differences in model errors
683 were unimportant.